

United States Department of Commerce
Technology Administration
National Institute of Standards and Technology

NIST Technical Note 1365

**Sub-Doppler Frequency Measurements
on OCS at 87 THz (3.4 μm)
with the CO Overtone Laser:
Considerations and Details**

A. Dax
J.S. Wells
L. Hollberg
A.G. Maki
W. Urban

QC
100
.U5753
NO. 1365
1994

**Sub-Doppler Frequency Measurements
on OCS at 87 THz (3.4 μm)
with the CO Overtone Laser:
Considerations and Details**

A. Dax*
J.S. Wells
L. Hollberg
A.G. Maki
W. Urban*

Time and Frequency Division
Physics Laboratory
National Institute of Standards and Technology
325 Broadway
Boulder, CO 80303-3328

*Institut für Angewandte Physik
der Universität Bonn
Bonn, D-53115 Germany

July 1994



**U.S. DEPARTMENT OF COMMERCE, Ronald H. Brown, Secretary
TECHNOLOGY ADMINISTRATION, Mary L. Good, Under Secretary for Technology
NATIONAL INSTITUTE OF STANDARDS AND TECHNOLOGY, Arati Prabhakar, Director**

National Institute of Standards and Technology Technical Note
Natl. Inst. Stand. Technol., Tech. Note 1365, 32 pages (July 1994)
CODEN:NTNOEF

U.S. GOVERNMENT PRINTING OFFICE
WASHINGTON: 1994

For sale by the Superintendent of Documents, U.S. Government Printing Office, Washington, DC 20402-9325

CONTENTS

	page
1. INTRODUCTION	2
2. THE NIST OVERTONE LASER	3
2.1 Sub-Doppler Experiments with the CO Overtone Laser	3
3. SATURATED-ABSORPTION CONSIDERATIONS	4
3.1 A Novel Linear Diode	4
3.2 Polarization Considerations	6
3.3 Experimental Results	8
4. OPTICAL HETERODYNE POLARIZATION SPECTROSCOPY	10
4.1 Analysis of OHPS Technique	10
4.2 Details of OHPS Experiment	12
4.2.1 The Two Stage Analyzer	12
4.2.2 The Compound $\lambda/4$ Plate	14
4.3 Elimination of Spurious Signals	15
4.4 Suitable Dispersion Signals	15
5. THE CO ₂ LASER SYNTHESIZER	17
5.1 Improvements in NIST CO ₂ Lasers	17
5.2 Synthesizer-CO Overtone Laser Beatnote	17
6. RESULTING HETERODYNE FREQUENCY MEASUREMENTS	18
7. ACKNOWLEDGMENTS	20
8. REFERENCES	21

Sub-Doppler Frequency Measurements on OCS at 87 THz
(3.4 μm) with the CO Overtone Laser: Considerations and Details

A. Dax†, J.S. Wells, L. Hollberg, and A.G. Maki‡

Time and Frequency Division
National Institute of Standards and Technology
Boulder, Colorado 80303

and

W. Urban
Institut für Angewandte Physik
der Universität Bonn
Bonn, D-53115 Germany

We have investigated two techniques for making sub-Doppler frequency measurements with the CO overtone laser. We studied three OCS transitions whose frequencies overlap either directly with CO $\Delta v = 2$ overtone transition frequencies or with the overtone lines after they have been shifted by an acousto-optic modulator. We have investigated both conventional saturated-absorption and an optical heterodyne polarization. While we eventually used the latter technique for our measurements, it is too cumbersome to use as a conventional laser stabilization tool. Saturation absorption is considerably simpler and has potential for a more accurate measurement, if some technical problems are overcome. This becomes more important in the light of a potential use of the CO $\Delta v=2$ $P_{26}(9)$ transition in a new frequency chain. This transition was used for the OCS $P(27)$ $10^0 1-00^0 0$ measurement. Polarization spectroscopic techniques with optical heterodyne detection were used to observe the features and then to provide the discriminant for locking the overtone laser to the OCS transitions. A CO_2 laser synthesizer was used for the frequency measurement basis. The new frequencies (uncertainties in parentheses) resulting from the measurements are for the OCS $10^0 1-00^0 0$ $P(27)$, 87 117 278.492(50) MHz; OCS $11^1 1-01^1 0$ $R(14)$, 87 222 001.143(70) MHz; and for the OC^{34}S $10^0 1-00^0 0$ $P(9)$, 87 010 586.671(75) MHz.

†guest researcher from
Institut für Angewandte Physik
der Universität Bonn
Bonn, D-53115 Germany

‡permanent address:
15012 24th Ave. SE
Mill Creek, WA 98012

Key words:

absolute frequency, measurements, carbonyl sulfide, frequency calibration standards, optical polarization spectroscopy, saturated absorption spectroscopy, sub-Doppler frequency measurements

1. INTRODUCTION

Since 1979, we have been involved in a major effort to provide frequency/wavenumber calibration standards based on heterodyne frequency measurements [1,2]. Our heterodyne frequency measurement activity came to a temporary halt when we reached the 61.76 THz (2060 cm^{-1}) region, the upper limit of our $\Delta v = 1$ CO laser [3]. Some measurements at slightly higher frequencies were possible based on a doubling of the CO₂ laser [4]. It was the development of the CO overtone laser [5] that made further progress possible. The most recent status [6] (over 330 transitions in the 2.6 to 4.1 μm region) suggests the potential usefulness of this laser. A long standing NIST-IAP collaboration resurfaced in Bonn, where the overtone laser served as a transfer oscillator in some tunable diode laser (TDL) based heterodyne measurements. Frequencies were measured of OCS transitions in the $11^{1e}1-01^{1e}0$ and $11^{1f}1-01^{1f}0$ bands at 87 THz (3.4 μm) [7]. With the exception of some measurements on CO [8] and N₂O [9], our measurements between 1979 and 1990 were all Doppler-limited. In a separate effort, Fayt et al. [10] have made sub-Doppler measurements on those OCS transitions that are near the 9 μm CO₂ laser transitions.

The Doppler-limited frequency measurements culminated in the publication of a calibration atlas [2] which spans much of the region from 486 to 3120 cm^{-1} plus another small region from 4071 to 4352 cm^{-1} . The atlas has a spectral map and facing table format and will be updated from time to time in the form of a computer diskette for the facing tables as new and improved frequency values become available [2,11]. Since a deliberate effort was made to keep the atlas at a manageable length, about three quarters of the possible frequency entries were not included. The diskette in NIST Standard Reference Database 39 includes these omitted values.

In an effort to further improve the calibration frequencies, both NIST and the IAP in the University of Bonn, Germany have started to make sub-Doppler frequency measurements on OCS. Our measurements were at 3.4 μm , those of our colleagues in Bonn were near 5 μm [12]. In this technote we describe the first NIST OCS experiments and the new frequency calibration tables appear elsewhere [13].

2. THE NIST OVERTONE LASER

The dc-gas-discharge-excited, CO-overtone laser was developed by W. Urban and co-workers at the Institut für Angewandte Physik (IAP) der Universität Bonn [5] and the current description of status and recent improvements is available in Ref [6]. Basically, this liquid-nitrogen-cooled flowing-gas CO laser operates on $\Delta v = 2$ transitions. It operates over the 2.6 μm to 4.1 μm region where some 330 lines have been made to lase. In our NIST laboratory we have constructed a CO overtone laser similar to the laser developed in Bonn [5]. Our 1.87 m long laser has a 450 line/mm grating and a 10 m radius-of-curvature output coupler. The LN_2 -cooled gain section is about 1.09 m long, with a bore ID of 12 mm. The operating partial pressures of the He, N_2 , air, and CO are essentially the same as the Bonn papers indicate [5,6]. (We can attest to the wisdom of using an aluminum gas cylinder for storing the CO to avoid problems [6] arising from $\text{Fe}(\text{CO})_5$ in older iron cylinders.) Our pressures were measured at the gas outlet of the laser under operating conditions (77 K, 4 ma discharge current). The partial pressures of the gases were: for helium, 844 Pa (6.35 Torr); nitrogen, 80 Pa (0.6 Torr); air, 6 Pa (0.05 Torr); and carbon monoxide, 53 Pa (0.4 Torr). The pumping speed of the effluent through the vacuum pump was about 1 ℓ/min at ambient temperatures and altitude.

The Bonn versions of the laser have the output power taken from the zeroth order of the grating. While our grating mount has a capability for such coupling, we chose to take the output from a dielectric-coated ZnSe coupler. This compensated coupler (the second surface of the coupler is curved) minimizes the spreading of the output beam. In an effort to minimize the laser linewidth, we have inserted convection barriers to enclose the regions between the resonator optical elements and the Brewster windows of the gain tube. We have also inserted a surge reservoir between the mixing valves and the gas inlet to the laser tube to reduce the effect of pressure fluctuations from the flow meters. For the lines used here, we have obtained single mode laser powers of 80 to 100 mW. The measured linewidth is about 100 kHz, and the measured polarization quality ($I_{\text{hor}}/I_{\text{vert}}$) was 2000.

2.1 *Sub-Doppler Experiments with the CO Overtone Laser*

Our experiment was designed to take advantage of the CO overtone laser to make some heterodyne frequency measurements with sub-Doppler techniques (and polarization sensitive devices) [14-47] on OCS transitions that overlap or nearly overlap a CO laser transition. Two

different experimental approaches were investigated to see which was best for making sub-Doppler measurements on the OCS transitions. The first involved saturated-absorption techniques [14-18,20,22,23], and the second used polarization-selective optical-heterodyne techniques [24,28-37,40,43-47]. The first technique is potentially the more accurate for frequency measurements [15-18] (provided that the transition moment of the molecule is sufficiently large) and is also much simpler to use. However, because of the weak transition moment involved and some technical problems in obtaining a clean modulation signal for third-derivative detection [28,29] this technique was shelved for the time being. The second technique produced a much better signal-to-noise ratio (SNR), but was considerably more cumbersome. We discuss details of both experiments showing their advantages and limitations.

3. SATURATED-ABSORPTION CONSIDERATIONS

The goal of optical heterodyne frequency measurements on calibration gases is to find precise line center positions. Despite the convenience and promising features which are afforded by an intracavity absorption cell [14], we have chosen an extracavity absorption cell. The extracavity operation promises better frequency accuracy of the molecular line to be measured by controllable pump/probe intensities and negligible gas lens effects [15,16].

3.1 *A Novel Linear Diode*

In order to stabilize a laser to a highly reproducible saturation feature, it is desirable to obtain a discriminant with both a high (SNR) and a small linewidth. The factor limiting the linewidth in a saturated-absorption experiment is often the residual Doppler width [17]. This arises from a small angle (which is usually introduced to prevent optical feedback to the laser) between the probe beam and the counterpropagating pump beam in the low pressure absorption cell. The common trick to prevent optical feedback and still have collinear beams is to insert an optical diode [18]. We present the features of the optical diode we used; it is a novel, simple, and broadband device. A comparison is made between our linear diode and the most commonly used diode in the mid-infrared, a linear polarizer in front of a $\lambda/4$ retarder plate [15,18] which we call a circular diode.

The principal setup of our saturated-absorption experiment is shown in Fig. 1. A three-mirror wavelength-independent polarization rotator rotates the horizontal polarization of the

incident laser beam to a 45° position [19]. After passing the polarizer, the single laser beam is split into two beams with equal intensities and high quality polarizations. One is parallel to and the other is perpendicular to the horizontal plane. As long as both beams have equal intensities and the beam paths are nearly equal in length, one tends to observe symmetric line shapes [20]. After one round trip, the ordinary beam enters the polarizer where the extraordinary beam has left it before. But now the ordinary beam stays ordinary (fixed by its polarization) and passes straight through the polarizer, where it can be focused on a detector.

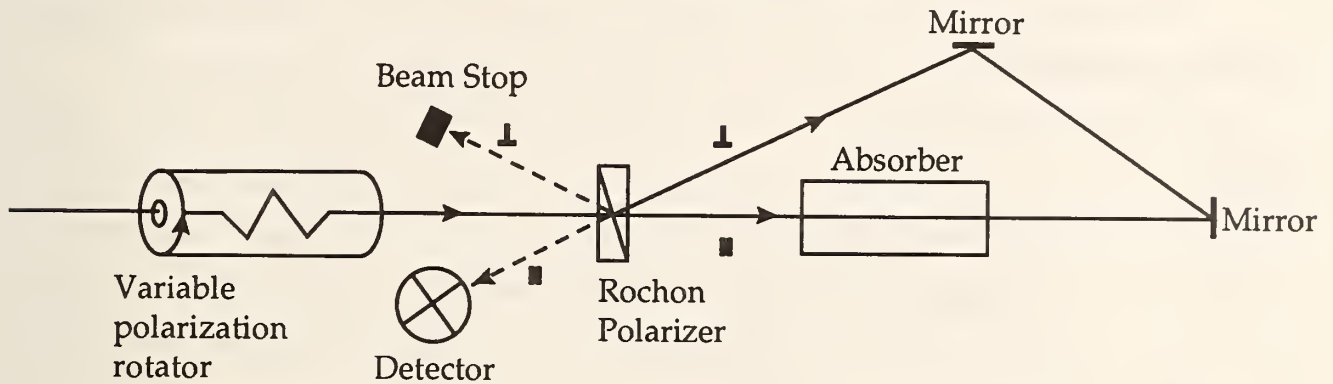


Figure. 1. Elements of setup for saturated absorption spectroscopy using a linear diode.

Conversely, the extraordinary beam separates in the opposite direction and can be focused to a second detector or beam stop.

Our polarizer was of a Rochon type made of MgF_2 [21]. We used the astigmatism-free ordinary beam for probing and the extra-ordinary beam for pumping. During the round trip, the plane of incidence at each optical component remains the same for both beams and their polarizations stay parallel and perpendicular to this plane. Therefore, no ellipticity which would considerably decrease the diode's quality can build up at reflective optical components.

An optical diode which used two birefringent crystals for linear polarizations has been demonstrated [22]; we have shown that a single crystal is sufficient. It is instructive to consider the difference in the expected saturated absorption signal strength between that produced with a linear diode and that from a circular diode.

3.2 Polarization Considerations

The molecular absorption cross section depends on the polarization of the applied laser beam [23,24]. This can be understood quantum mechanically by a different overlap of the m -dependent wave functions related to a molecular transition expressed by the relevant Clebsch-Gordon coefficients [23]. Classically, this effect is attributable to the fact that a light field rotating in the same sense as the spinning molecule undergoes a pronounced interaction [25]. Thus, the saturation of a molecular transition depends on the polarization of the laser beam, the rotational quantum number J , ΔJ , and the magnetic quantum number m .

The absorption coefficient α_p for the probe beam in the limit of weak saturation is generally given [25] by

$$\alpha_p = \alpha_0 - \beta_p I_p - \theta_{ps} I_s, \quad (1)$$

where

- α_0 = linear absorption coefficient,
- β_p = self saturation coefficient for the probe beam,
- θ_{ps} = cross saturation coefficient,
- I_p = probe beam intensity,
- I_s = pump beam intensity.

θ_{ps} describes the interaction between the pump and probe beam transferred by the nonlinear optical medium. It is responsible for a Lamb dip on the Doppler profile given by the linear absorption coefficient α_0 .

The polarization dependence has already been extracted from θ_{ps} by Dabkiewicz and Hänsch et al. [26,27]. They have taken advantage of the Wigner-Eckart theorem and have summed the Clebsch-Gordon coefficients over the magnetic quantum numbers. They obtained four relevant factors $\zeta_{JJ'}^+$, $\zeta_{JJ'}^-$, $\zeta_{JJ'}^{\parallel}$, and $\zeta_{JJ'}^{\perp}$, describing the polarization dependent interaction of the counterpropagating pump and probe beams. Here J is the lower state and J' the upper state rotational number of the corresponding molecular transition. ζ^+ stands for two circularly polarized beams spinning in the same direction, ζ^- for two circularly polarized beams spinning oppositely, ζ^{\parallel} for two parallel linearly polarized, and ζ^{\perp} for two perpendicular linearly polarized beams.

Their calculation is restricted to the following limitations:

1. Weak saturation,
2. Natural linewidth \ll doppler width,
3. Spontaneous emission is neglected,
4. No multiple optical pumping, and
5. No coherence effects (already included in 2).

To get appropriate information about the signal strength by using different optical diodes, we need to know whether the above cited ζ are comparable and which ζ values correspond to which experimental setup.

The comparability of the factors ζ is discussed in References [23] and [24], which show that we have to refer all ζ 's to one saturation intensity. In Ref. [24] this is the saturation intensity for the case where two counterpropagating beams are polarized linearly and are parallel to each other. That has already been accomplished in the same way by Dabkiewicz and Hänsch [26]. So we obtain, for example, for large J values ($J \geq 4$) the scaling law: $\zeta^+ : \zeta^- : \zeta^\perp : \zeta^\parallel$ scale as $3/2 : 1/4 : 3/4 : 1$ for R and P transitions and as $2/3 : 2/3 : 1/3 : 1$ for Q transitions.

The second problem concerns only the circularly polarized case. For convenience the circularly polarized beam passing the circular diode is normally retroreflected somewhere behind or inside the gas sample cell (see for example Ref. [15]). Therefore, we have for that case the situation depicted in Fig. 2. A σ^+ polarized beam is going to the right and a σ^- polarized beam to the left. Since both have the same spinning direction, ζ^+ is the appropriate parameter here.

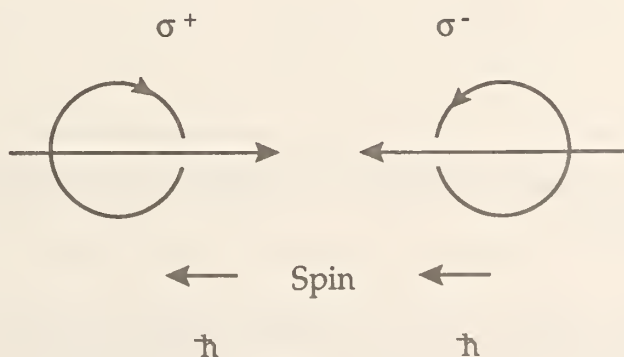


Figure 2. The two counterpropagating σ^+ and σ^- beams are spinning in the same direction.

So the saturated absorption signal (in the limit of small saturation and $J > 4$) is two times larger when we use a circular diode with a retroreflector behind than when we use our linear diode.

If necessary, we can recover the factor of two by summing up the two detector signals mentioned above. A linear diode based on the Faraday effect [18] would lead to a $2/3$ times smaller signal for R and P transitions compared to using a circular diode and a $3/2$ times larger signal for Q transitions.

3.3 Experimental Results

We set up a slightly more complex experiment than Fig. 1 suggests; the primary difference was that we attenuated the power down to about 1 mW in each beam. Figure 3 shows a recorded Lamb dip employing this setup. The laser was frequency modulated by applying a 1.2 kHz sine wave to a single piezoelectric transducer (PZT) on the laser mirror mount. The Lamb dip was obtained by detecting at $3f$ (3.6 kHz) [28,29] and scanning the laser frequency over the absorption profile. The gas pressure in the 1.5 m long absorption cell was 0.27 Pa and the laser power approximately 1 mW for each beam. The SNR was 14 and the linewidth of this $P(27)$ $10^0 1-00^0$ transition was less than 200 kHz.

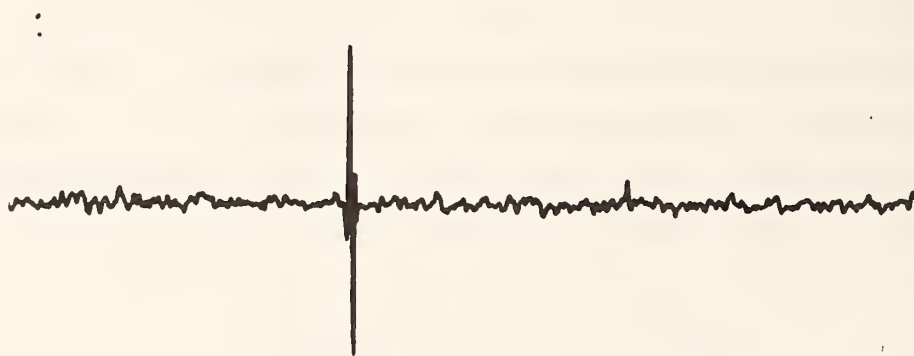


Figure 3. The third derivative saturated absorption signal of the OCS $P(27)$ line at $3.4 \mu\text{m}$. The linewidth is less than 200 kHz.

Despite this promising result, which can be improved by using more laser power in the cell, we rejected this technique for two technical reasons. The first is a problem with the PZT which had nonlinearities and a slight tilt with increasing voltage. The nonlinearity often caused the Lamb dip to appear asymmetric. The second reason for rejecting this technique was that the

liquid-nitrogen-cooled CO overtone laser shows randomly distributed intensity spikes after a few hours of operation (Fig. 4).



Figure 4. Randomly distributed intensity spiking of the CO overtone laser after a few hours of operation. The detection system and experimental parameters are the same as for Fig. 3.

Obviously, this limits the accuracy of stabilizing a laser to a reference line. The reason for this spiking is attributable to frozen CO_2 particles falling down the laser tube wall and crossing the laser beam. CO_2 is built up from dissociation products of CO in the gas discharge exiting the laser active medium. This can be a problem for this laser (and for the $\Delta v = 1$ CO laser running on high vibrational quantum numbers) since a relatively high amount of CO (up to 8 percent) is necessary to run these lasers [6,30].

Our quasi-wavelength-independent setup has been adopted by our colleagues in Bonn [12,31] for calibration gas measurements at $5 \mu\text{m}$. They had much higher (about 1000 time higher) spectral line intensities for most of their measured OCS and CO transitions and no spiking problem due to the low amount of CO in their $5 \mu\text{m}$ CO laser. Alternatively, they employ a Cardanic-compensated PZT and mirror mount similar to Ref. [32] originally designed for the Bonn CO_2 lasers [33,34] and a still higher modulation frequency using a two-stage PZT [35,36].

4. OPTICAL HETERODYNE POLARIZATION SPECTROSCOPY

The polarization spectroscopy method was invented by Wieman and Hänsch in 1976 [37]. Since then, this versatile method has been used not only for several laser spectroscopic measurements, but also for laser stabilization [38-47]. The principle of operation is that a strong pump beam introduces an anisotropy in a sample; that is, the sample becomes dichroic and birefringent if the pump frequency is near a molecular resonance. A weak probe beam at the same frequency will suffer a change in its polarization if it interacts with the same molecules as the pump beam. With an appropriate selection method, we can observe these changes in polarization at low power. The possible variations concerning the polarization of the pump and probe and the offset angle of the analyzer from a predetermined orientation produce different signal shapes and intensities for molecular Q , R , and P transitions [37-42].

After the problems with the saturated absorption technique, we selected the optical heterodyne polarization spectroscopy (OHPS) technique [24,37,43]. Its physical principle is extensively explained in Ref. [44].

4.1 Analysis of OHPS Technique

The main advantage of the OHPS technique is that a weak signal can be considerably enhanced by heterodyning the signal wave (amplitude E_s) with a much stronger local oscillator wave (amplitude E_0), as long as E_0 (which can also contribute noise) is selected appropriately. To use this technique, we apply intensity modulation to the pump beam and detect the modulation transfer to the probe beam. The result is a low noise dispersion shaped signal which depends on the molecular transition. This sub-Doppler signal is appropriate for the stabilization (a line-center-lock to a molecular transition) of a laser. An absolute frequency measurement of the stabilized-laser radiation can then permit the molecule to be used for calibration. The J dependence of the signal is calculated in Refs. [24],[37],[40], and [43].

Since both birefringence and dichroism can contribute to the signal here, the most difficult problem is to obtain a line shape that is symmetric about the true line center [37,45,46]. The local oscillator wave E_0 can be obtained most conveniently from the probe beam itself by slightly uncrossing the analyzer with respect to the polarizer by an angle ϕ . An improper choice of ϕ may be accompanied by asymmetries in the dispersion signal.

It is of interest to consider the SNR for this type of experiment in the infrared region.

Workers in the visible region use the approximation $\text{SNR} \approx 1/\xi$, where ξ is the extinction ratio of the analyzer. The detector noise, however sets a finite limit. In the visible (500 nm), the detector noise may be 10^{-5} that of the detectors in the $3 \mu\text{m}$ region [49], and we may assume that $D_r \ll \gamma P_0$, where γP_0 is the laser noise and P_0 is the laser output power. In this case, the detector noise may be neglected. The detector noise may not be neglected in the $3 \mu\text{m}$ region.

Let $\Delta\phi$ be the azimuth angle change of the probe beam's polarization vector due to the birefringence of the medium. As shown in the section following Eq. (3), $\Delta\phi$ is proportional to $\Delta n k_0 L$, where Δn is the refractive index change, k_0 is the wavevector, and L is an effective path length. We detect changes in the azimuthal angle which produce a signal, $S = 2P_0\Phi_1\Delta\phi$, where Φ_1 is the offset angle of the analyzer. We consider for now a single-stage analyzer. The laser power reaching the detector is $P_0(\Phi_1^2 + \xi)$, where $P_0\xi$ represents the leakage through the analyzer.

The laser noise is this term multiplied by γ , and since the detector and laser noise are uncorrelated, the total noise is given by $N = \{[\gamma P_0(\Phi_1^2 + \xi)]^2 + D_r^2\}^{1/2}$. To find the maximum value for the SNR (limited by the laser power [48]), we look for an extremum with respect to the variable Φ_1 . With the optimum value for Φ_1 we obtain

$$\text{SNR}_{\max} = \text{Const} [P_0/(\gamma D_r)]^{1/2}, \text{ for } \gamma P_0\xi \ll D_r. \quad (2)$$

A good extinction ratio of the analyzer is essential. In the visible spectral region extinction ratio values of 10^{-7} are often cited [37,47]. Our Rochon type analyzer had a specified extinction ratio of $\xi = 10^{-5}$ [21]. Practically, it is not that good because of the optical beam path through the crystal (the crystal is often tilted to avoid feedback to the laser).

By using a two-stage analyzer we could improve the extinction ratio considerably. By using the Jones formalism [50], we have calculated the contributions to the detector response I_{det} and achieved, by using linear approximations

$$\begin{aligned} I_{\text{det}} = & C e^{-\kappa k_0 L} E_0^2 \{ \xi_1 \xi_2 - \xi_1 \epsilon^2 - \xi_2 \epsilon^2 + \epsilon^2 - \epsilon k_0 \Delta b_i + \phi_1^2 + \phi_1 k_0 \Delta b_r - \epsilon \Delta \kappa k_0 L + \phi_1 \Delta n k_0 L \\ & + 1/2 [k_0^2 \Delta n L \Delta b_r + k_0^2 \Delta \kappa L \Delta b_i] \\ & + 1/4 [(k_0 \Delta n L)^2 + (k_0 \Delta b_r)^2 + (\Delta \kappa k_0 L)^2 + (k_0 \Delta b_i)^2] \} \end{aligned} \quad (3)$$

where C is a proportionality constant, κ is the susceptibility ($\kappa = \kappa_+ + \kappa_-$), $k_0 = 2\pi/\lambda$, λ is the wavelength of the probe beam, and L is the estimated overlap length of the crossed beams within the cell. The symbols ξ_1 and ξ_2 represent the extinction ratios for the first and second analyzer, ϵ is the ellipticity of the polarization after the polarizer, and $\Delta\kappa = \kappa_+ - \kappa_-$ and $\Delta n = n_+ - n_-$ are the susceptibility change and refractive index change of the anisotropic medium in the circular basis. $\Delta\kappa$ describes the dichroism having a Lorentzian lineshape, Δn describes the birefringence and has a dispersion lineshape, ϕ_1 is the deviation from the crossing angle of the first analyzer, and $\Delta b_r = b_r^+ - b_r^-$ (the real part) and $\Delta b_i = b_i^+ - b_i^-$ (the imaginary part) describe the anisotropy of the cell windows under vacuum stress [24,28,43].

Since both extinction ratios have similar values between 10^{-4} and 10^{-5} , the term $\xi_1\xi_2$ is negligible. The same is usually true for all terms containing ϵ^2 , since we have found experimentally that $\epsilon < 10^{-3}$. The signal term can be expressed as $\phi_1 E_0 (E_0 \Delta n k_0 L)$, showing the heterodyning of the signal amplitude $E_0 \Delta n k_0 L$ and the local oscillator amplitude $\phi_1 E_0$ [44]. The terms $\Delta\kappa$, $(\Delta\kappa)^2$, and $(\Delta n)^2$ may lead to asymmetry of the signal, and the remaining terms are responsible for the background.

4.2 Details of the OHPS Experiment

The overtone laser is the starting point of the experiment in the block diagram in Fig. 5. The output of the overtone laser is directed by several mirrors to a wedged, uncoated ZnSe beam splitter where the transmitted portion is used for the saturating beam. The beam reflected from the front surface is used for the linear probe beam, and the beam reflected from the back surface is directed via an acousto-optic modulator to the IR frequency synthesizer. When a frequency overlap did not exist between the CO and OCS transitions, the beam from the overtone laser traversed the AOM first (for a shift to the required frequency) and then onto the three functional paths.

4.2.1 The Two Stage Analyzer

As indicated in Fig. 5, the probe beam's polarization was rotated by $\pi/2$ by the five-mirror variable rotator and was then focused by mirror 1 onto a reflecting wedged germanium plate polarizer [33,51]. The beam is recollimated by mirror 2. This increases the polarization purity of the beam from 2000:1 at the laser output to greater than 650 000:1. A four-mirror polarization-conserving half-wave plate [33,52] returns the polarization back to horizontal. The

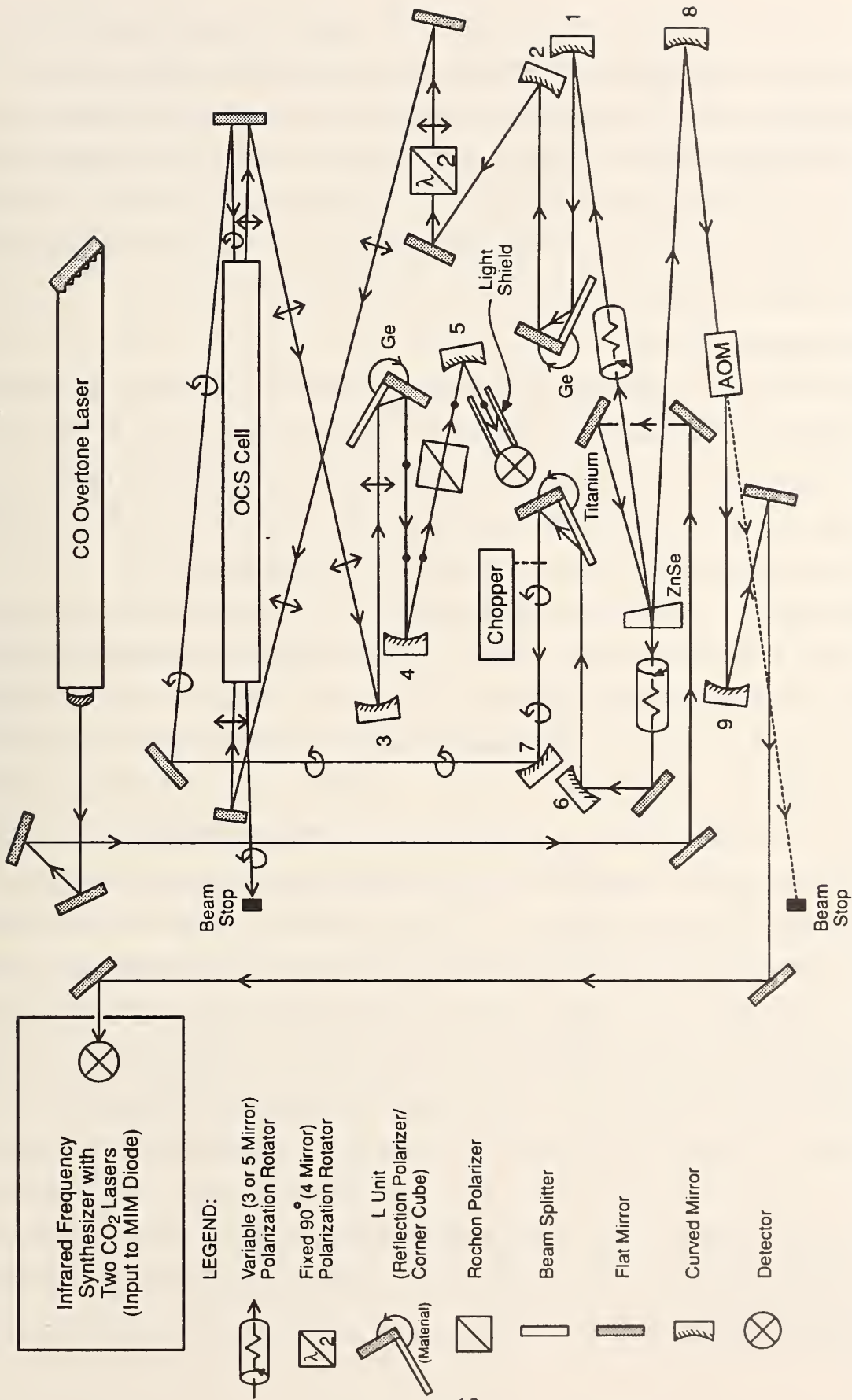


Figure 5. Functional diagram for sub-Doppler frequency measurements on the P(27) line in the OCS 10⁰1-00⁰0 band at 3.4 μm.

probe beam traverses the OCS cell at a small angle with respect to the cell axis and is focused by mirror 3 onto a second reflecting wedged germanium plate polarizer which acts as the first stage of the analyzer. Only the component polarized perpendicular to the plane of incidence is reflected by this L unit along on the detection path. The local oscillator wave is generated by tilting the base of this device to the offset angle ϕ_1 . A similar one stage analyzer can also be found in Refs. [38] and [48]. These collinear signal and local oscillator beams are focused on the Rochon analyzer by mirror 4 and mirror 5 focuses them on the detector.

4.2.2 The Compound $\lambda/4$ Plate

Before considering the path of the pump beam, we point out that instead of the usual $\lambda/4$ plate, we have used a two-component scheme to achieve circular polarization. Our two-component scheme has two advantages. First, and most important, it is possible to have control over the polarization quality (similar to using a Babinet-Soleil compensator). Additionally, the device is purely reflective and consequently is nearly wavelength independent.

The path (shown in Fig. 5) of the saturating beam through our two-component device starts where it emerges from the ZnSe beam splitter. The beam then has its polarization rotated by a three-mirror variable polarization rotator to some arbitrary value, say Φ (the difference between a three-mirror rotator and a five-mirror rotator is that the latter conserves the polarization quality much better [33]). The beam is focused by mirror 6 on a titanium plate, which affords an adjustable angle Θ of incidence relative to the incoming beam. The physics involved in the phase shift on reflection from the titanium plate is described in [33] and is simply the physics of Fresnel reflection by a metal surface [53]. A measured polarization quality of 99.5 percent was achieved for the saturation beam by iterative adjustment of the angles Φ and Θ . It is essential to have a good circular polarization quality here, otherwise the pump wave can be considered to be composed of a circular and a linear part where dichroism can be accompanied with this linear pump wave. According to Ref. [38] such a dichroism changes the azimuthal angle of the probe beam's linear polarization. The resulting absorption-shaped contribution to the signal would increase, making the dispersion-shaped signal asymmetric relative to the baseline and relative to the baseline intersection point. The saturation beam traversed the cell at a small angle with the cell axis. The crossing angle between the two beams was estimated to be about 1 mrad.

4.3 Elimination of Spurious Signals

The experiments required a major rearrangement of our laboratory. The area available for the saturation scheme was rather small (1 m \times 2.5 m) and a considerably larger number of folding mirrors was used than Fig. 5 would suggest. This led to some complications, since even a minuscule reflection from the perimeter of the beam could somehow find its way back to the sensitive detection system. Determining sufficient clearances for the beam was a tedious procedure. The problem of interfering noise by backscattered pump light and the leaking probe light at the detector has already been pointed out in Ref. [37]. The recommended solutions are to use a spatial filter [24,37], an intermodulation technique [46], or a phase modulation of the pump beam [43], or to shift the frequency between the pump and probe beam [47].

By greatly increasing the gain of the detector amplifier we found two ways to reduce the background signal and a third procedure to reduce the background interference noise more than 2 orders of magnitude. Besides spatial shielding in front of the detector, we cleaned all mirrors and made them meticulously free of dust before each measurement. In addition, almost the whole optical path was flushed with dry nitrogen gas. This was very effective, since interference noise is attributable to random fluctuations of the refractive index caused by air turbulence in the probe and pump beam path. This flushing removed CH₄ and water which are atmospheric absorbers at 3.4 μm [54].

4.4 Suitable Dispersion Signals

When the elimination of the spurious signals was completed, suitable stabilization signals were observed. We measured the frequency of three OCS transitions which had accidental overlaps with the CO overtone laser or its AOM shifted sidebands. Some of the data from the experiment on the *P*(27)A line of OCS at 3.4 μm are shown in the next two figures. Figure 6 shows the nearly symmetric dispersion signal which was used to lock the CO overtone laser. The common procedure for achieving a symmetric signal is to squeeze the cell windows in order to reduce the term $k_0^2 \Delta \kappa L \Delta b_i / 2$ (see Eq. (3)). This is the main contribution to the asymmetry of the signal if $\epsilon \ll k_0 \Delta b_i$.

We investigated an alternative method which was to rotate the second analyzer (Rochon crystal) of our two stage system relative to the first analyzer. Offset angles of $\phi_2 < 5^\circ$ were enough to achieve symmetric signals. Since the polarization of the probe beam after the first

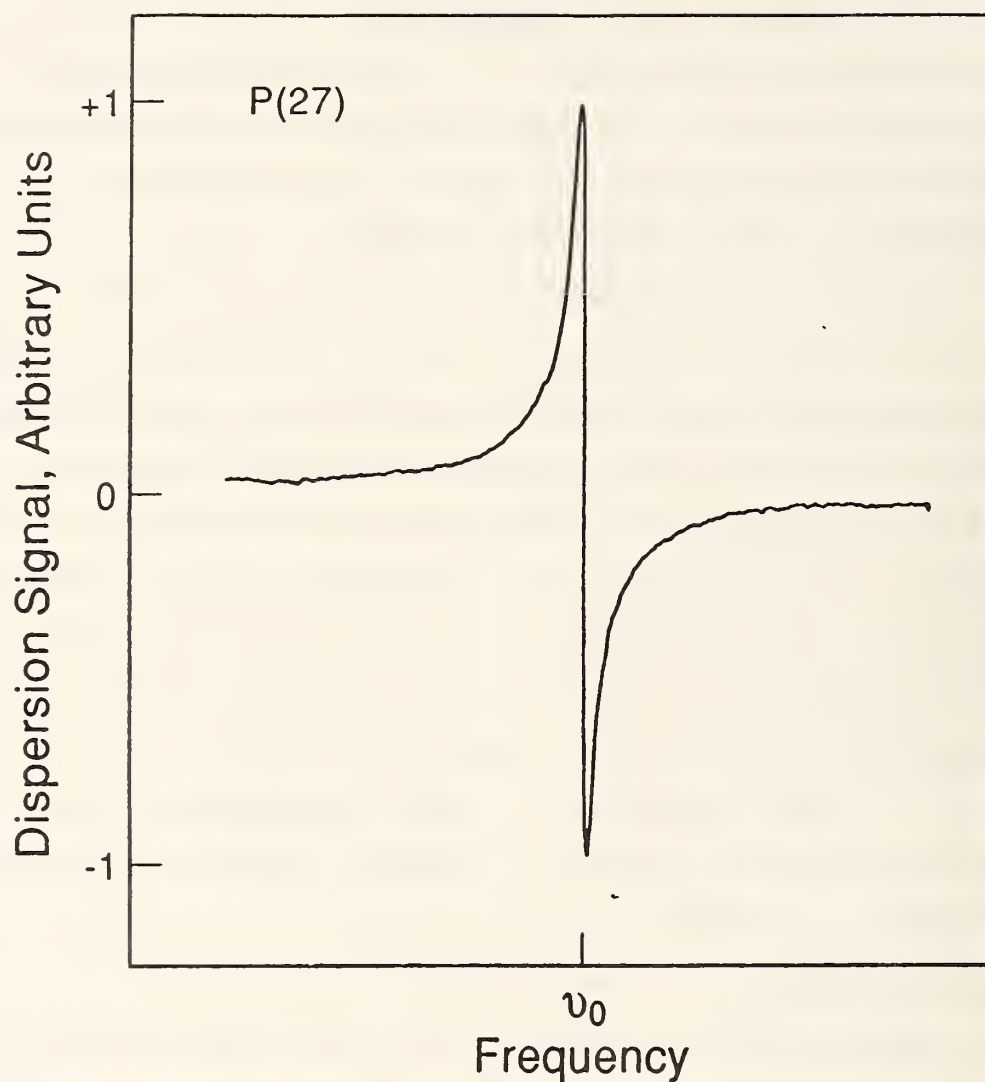


Figure 6. Dispersion signal of saturated $P(27)$ OCS transition. The center frequency is 87 117 278.492(50) MHz and the peak to peak linewidth is about 700 kHz. The width of the scan shown here is about 45 MHz.

analyzer is elliptical, this technique is reminiscent of the method employed by Delsard and Keller [39]. They used a linear pump beam and a circular probe beam and found that it was possible to change the signal continuously from an absorption shape to a dispersion shape simply by rotating their analyzer 45° .

Our quantitative description does not demonstrate that we can symmetrize the signal without changing the real zero crossing of the Lamb dip. To do this would require the inclusion of a valid model which describes the cell windows under stress. However, not only do the dispersion signals appear symmetric, but also another measurement using a different technique produced a result which agreed to within 20 kHz with our result for the same 5.3 μm OCS transition [12,13,55].

5. THE CO₂ LASER SYNTHESIZER

We refer again to Fig. 5; the third beam from our wedged ZnSe beamsplitter was focused by mirror 8 on the acousto-optic modulator (AOM), and the shifted beam was recollimated and sent to the input of the infrared frequency synthesizer. The frequency synthesizer consists of two CO₂ laser frequency standards, a microwave oscillator, a MIM diode, and a spectrum analyzer along with a marker oscillator. (See Ref. [2], pp. 17-21, or Refs. [3], [4], or [7].)

5.1 *Improvements in NIST CO₂ Lasers*

The CO₂ lasers in our synthesizer were previously used in less accurate measurements and are still stabilized with a first derivative lock. In order to upgrade the lasers and achieve higher accuracies, we have started our improvements by converting stabilization to an external cell (pressure 5.3 Pa (40 mTorr) CO₂). The output of each CO₂ laser was directed towards its own 85 percent reflecting ZnSe beam splitter and the reflected portions were directed to an external cell and retroflected at a small angle to avoid feedback to the laser. The transmitted portions were combined on a 50 percent beam splitter and directed to the MIM diode, which was also irradiated with the CO overtone laser power. Each laser was retrofitted with a new ribbed bore design gain tube to discriminate against off-axis modes. One CO₂ laser had invar support rods, the second one is currently being modified to include them. New locking-electronics and new PZTs will complete the improvement program.

5.2 *Synchronizer-CO Overtone Laser Beatnote*

Figure 7 shows the time-averaged beatnote between the locked CO overtone laser (after passing through the AOM) and a reference synthesized from a combination of CO₂-stabilized laser standards. Aside from the frequency determination, which is the primary goal, two features are significant. The first is that the linewidth of the laser is about 100 kHz, which is

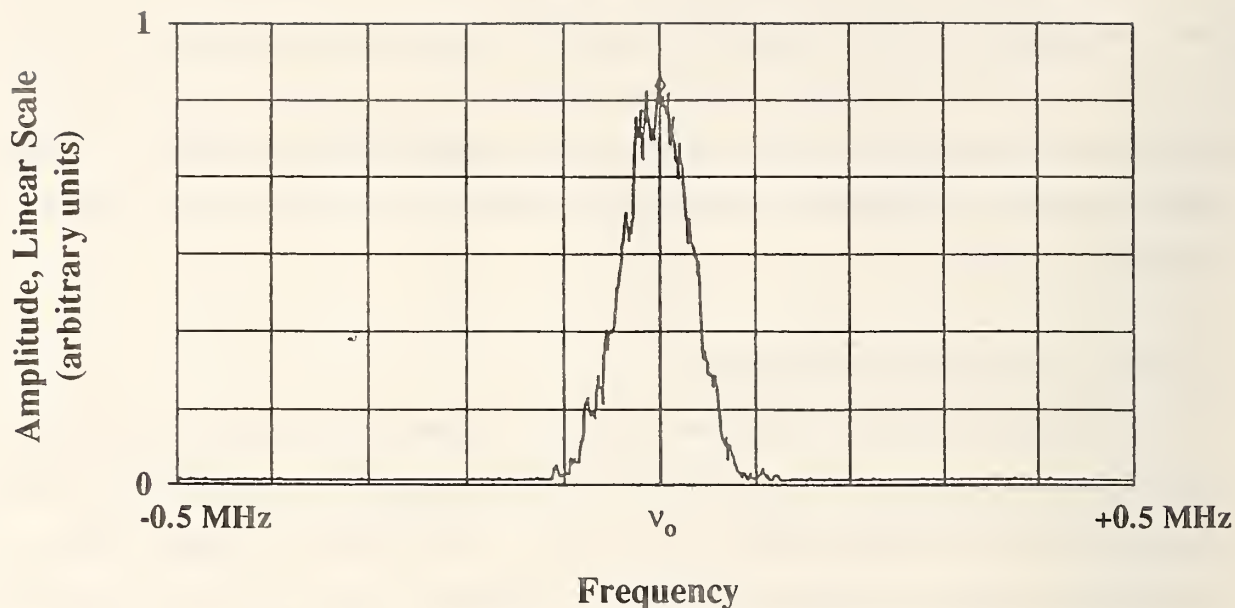


Fig. 7. Spectrum analyzer display of time-averaged (100 scans) beatnote between the CO overtone laser which was locked to the $P(27)$ line and a reference from the infrared frequency synthesizer. The center frequency is 1171.900 MHz, the video bandwidth is 30 kHz, and the sweep time is 62.56 ms.

considerably less than the 700 kHz saturation feature. The relative phase and amplitudes of modulation of the reference lasers were adjusted to minimize the beatnote linewidth; hence the linewidth here is an upper limit on that of the CO laser.

The second feature (not discernible here) is that the SNR of the beatnote was generally between 25 and 30 dB, and hence suitable for stabilizing the overtone laser to the synthesized reference. This makes it an ideal reference for use in a heterodyne measurement to measure the linewidth of TDLs and to use in frequency offset control in an alternate scheme with a line narrowed TDL [56].

6. RESULTING HETERODYNE FREQUENCY MEASUREMENTS

Dispersion signals similar to that in Fig. 6 were obtained for two other transitions. Parameters for these measurements were pressures of about 1.3 Pa (10 mTorr) with an estimated overlap pathlength L of about 1 m in a 1.5 m long absorption cell. The measurements were all

made with the same sample of gas at room temperature. No isotopically enriched samples (^{34}S for example) were used in the measurements. Table I gives the three sub-Doppler frequency measurements made through the use of this polarization spectroscopic technique. This technique is limited to the measurement of transitions that happen to be within the limited tuning range of the CO laser lines or within the range of the side-band produced by the acousto-optic modulator. The uncertainties in the measurements come from two sources. One is the uncertainty in locating the line center. Our estimate of this uncertainty comes from two sources. One is one half of the peak-to-peak frequency separation divided by the signal to noise ratio. The other part is one half of the peak-to-peak frequency separation divided by the signal to asymmetry ratio, where we define the asymmetry ratio as the difference between the midpoint of a line connecting the peaks and the extrapolation of the off axis baseline through the zero crossing of the discriminant. The second part of the uncertainty comes from possible deviations from locking the CO₂ lasers to the desired frequency. This can arise from less than optimal setting of the grating, DC offsets in the servo signal, and drifts in the offset that occur after initially zeroing out such errors. Based on some locking studies, we think this could be as high as 10 kHz for

Table I. The measured transition frequencies for carbonyl sulfide.

CO Trans. ^a	OCS Transition	Obs. Freq. ^b (MHz)	CO ₂ Freq. Stds. ^c	Beat Freq. (MHz)
$P_{26}(9)$	$P(27)$ 10^01-00^00	$87\ 117\ 278.496 \pm 0.050$	$2 \times R(8)\text{I} + R(12)\text{I}$	-1261.908
$P_{26}(8)$	$R(14)$ $11^{1f}1-01^{1f}0$	$87\ 222\ 001.143 \pm 0.070$	$2 \times P(28)\text{I} + P(32)\text{II}$	-1056.507 ^d
$P_{26}(10)$	$P(9)^e$ 10^01-00^00	$87\ 010\ 586.667 \pm 0.075$	$2 \times R(28)\text{I} + P(24)\text{I}$	-412.438

^a For the CO laser designation the subscript indicates the lower state vibrational quantum number and the number in parentheses is J'' .

^b The OCS observed frequency is given by the sum of the CO₂ laser frequencies and the beat frequency.

^c For the CO₂ laser designation the I indicates the 10 μm band and the II indicates the 9 μm band.

^d For the measurement of the $R(14)$ line of the $11^{1f}1-01^{1f}0$ band a microwave frequency of 10 999.988 MHz was added to the CO₂ laser frequencies.

^e This transition is for $^{16}\text{O}^{12}\text{C}^{34}\text{S}$; the other two are for $^{16}\text{O}^{12}\text{C}^{32}\text{S}$.

each harmonic required for synthesis. The standard deviation of each measurement set was less than the estimated uncertainties, since some possible systematic errors are included in the estimated uncertainties.

The CO₂ laser frequencies used to calculate the measured OCS frequency values in Table I were taken from a recent reanalysis of the CO₂ laser frequencies [57] and, for the lines used for this work, only differ from the frequencies given by Bradley et al. [58] by a few kilohertz.

These new OCS frequencies were added to our 5700-entry data bank and fitted (each data point is weighted as the square of the reciprocal of the uncertainty) to determine new molecular constants. These constants were then used to predict new frequency calibration tables with smaller uncertainties than had existed previously. These tables appear in Ref. [13].

7. ACKNOWLEDGMENTS

This work was supported in part by the NASA Office of Upper Atmospheric Research. A. Dax was funded by the Deutsche Forschungsgemeinschaft and the Graduiertenkolleg "Wechselwirkung in Molekülen" in Bonn, Germany. The Institut für Angewandte Physik of the University of Bonn provided a large quantity of optics for this experiment. We thank B. Nelles and his co-workers from Carl Zeiss for polishing the titanium mirror and Koch from the Deutsche Titan GmbH Düsseldorf for making the substrate available to us. We also thank L. Zink of CIRES for valuable suggestions regarding this manuscript.

8. REFERENCES

1. Wells, J.S.; Petersen, F.R.; Maki, A.G.; Heterodyne frequency measurements with a tunable diode laser-CO₂ laser spectrometer: spectroscopic reference frequencies in the 9.5 μm band of carbonyl sulfide, *Appl. Opt.* **18**: 3567-3573 (Nov 1979).
2. Maki, A.G.; Wells, J.S.; Wavenumber calibration tables from heterodyne frequency measurements, *Natl. Inst. Stand. Technol. Special Publication* 821, 1991.
3. Wells, J.S.; Schneider, M.; Maki, A.G.; Heterodyne frequency measurements of OCS near 61.76 THz (2060 cm^{-1}), *J. Mol. Spectrosc.* **140**: 170-176 (Mar 1990).
4. Maki, A.G.; Wells, J.S.; Jennings, D.A.; Heterodyne frequency measurements of CO and OCS beyond 2100 cm^{-1} , *J. Mol. Spectrosc.* **144**: 224-229 (Nov 1990).
5. Gromoll-Bohle, M.; Bohle, W.; Urban, W.; Broadband CO laser emission on overtone transition $\Delta v=2$, *Opt. Comm.* **69**: 409-413 (Jan 1989).
6. Bachem, E.; Dax, A.; Weidenfeller, A.; Schneider, M.; Urban, W.; Recent progress with the CO-overtone $\Delta v=2$ laser, *Appl. Phys.B* **57**: 185-191 (Dec 1993).
7. Dax, A.; Mürtz, M.; Wells, J.S.; Schneider, M.; Bachem, E.; Urban W.; Maki, A.G.; Extension of heterodyne frequency measurements on OCS to 87 THz (2900 cm^{-1}), *J. Mol. Spectrosc.* **156**: 98-103 (Nov 1992).
8. Pollock, C.R.; Petersen, F.R.; Jennings, D.A.; Wells, J.S.; Maki, A.G.; Absolute frequency measurements of the 2-0 band of CO at 2.3 μm ; calibration standard frequencies from color center laser spectroscopy, *J. Mol. Spectrosc.* **99**: 357-368 (June 1983).
9. Pollock, C.R.; Petersen, F.R.; Jennings, D.A.; Wells, J.S.; Maki, A.G.; Absolute frequency measurements of the 00⁰2-00⁰0, 20⁰1-00⁰0, and 12⁰1-00⁰0 bands of N₂O by heterodyne spectroscopy, *J. Mol. Spectrosc.* **107**: 62-71 (Sept 1984).
10. Fayt, A.; LaHaye, J.G.; Lemaire, J.; Herlemont, F.; Bantegnie, J.G.; Waveguide and diode laser heterodyne measurements with CO₂ laser and assignment of the cw FIR laser emission of OCS, *J. Mol. Spectrosc.* **140**: 252-258 (Apr 1990).
11. Maki, A.G.; Wells, J.S.; New frequency calibration tables from heterodyne frequency measurements, *Natl. Inst. Stand. Technol. J. Res.* **97**: 409-470 (Jul-Aug 1992), and *Natl. Inst. Stand. Technol. Reference Database #39*, Wavelength calibration tables (1992).

12. George, T.; Wappelhorst, M.H.; Saupe, S.; Mürtz, M.; Urban, W.; Sub-Doppler heterodyne frequency measurements on carbonyl sulfide transitions between 56 and 62 THz, *J. Mol. Spectrosc.* (accepted).
13. Dax, A.; Wells, J.S.; Hollberg, L.; Maki, A.G.; Urban, W.; Sub-Doppler frequency measurements on OCS at 87 THz (3.4 μm) with the CO overtone laser, *J. Mol. Spectrosc.* (accepted).
14. Chebotayev, V.P.; Supernarrow saturated absorption resonances, *Physics Reports* 119: 75-116 (Mar 1985).
15. Clairon, A.; Acef, O.; Chardonnet, C.; Bordé, C.J.; State of the art for high accuracy frequency standards in the 28 THz range using saturated absorption resonances of OsO₄ and CO₂, A. de Marchi (ed.) *Frequency Standards and Metrology*, 212-221, Springer-Verlag, Berlin (1989).
16. Ghosh Roy, D.N.; Bertinotto, F.; Rebaglia, B.I.; Cresto, P.C.; Effects of iodine saturation dispersion on the ¹²⁷I₂ stabilized He-Ne laser, *J. Appl. Phys.* 54: 531-534 (Feb 1983).
17. Hirano, I.; Saturated absorption spectra on the Cs-D₂ line, *J. Quant. Spectrosc. Radiat. Transf.* 42: 359-373 (Nov 1989).
18. Levenson, M.D.; *Introduction to Nonlinear Spectroscopy*, Academic Press (1982).
19. Greniger, Charles E.; Reflective device for polarization rotation, *Appl. Opt.* 27: 774-776 (Feb 1988).
20. Hall, J.L.; Bordé, C.J.; Shift and broadening of saturated absorption resonances due to curvature of the laser wave fronts, *Appl. Phys. Lett.* 29: 788-790 (Dec 1976).
21. Bernhard Halle Nachf. GmbH & Co. Data sheet, Berlin Germany, (1991).
22. Couillaud, B.; in *Progress in Atomic Spectroscopy* in Beyer, Kleinpoppen, eds., Part C, Plenum Press (1984).
23. Sargent III, M.; Polarized field saturation spectroscopy, *Phys. Rev. A* 14: 524-527 (July 1976).
24. Teets, R.E.; Kowalski, F.V.; Hill, W.T.; Carlson, N.; Hänsch, T.W.; Laser polarization spectroscopy, *Proc. Soc. Photo-Opt Instrum. Engrs.* 113: 80-87 (Aug 1977).

25. Meystre, P.; Sargent III, M.; Elements of quantum optics, Springer-Verlag, Berlin (1990).
26. Dabkiewicz, Ph.; Hänsch, T.W.; Polarization intermodulated excitation (POLINEX) of the CuI 578.2 nm transition, Opt. Comm. 38: 351-356 (Sept 1981).
27. Hänsch, T.W.; Lyons, D.R.; Schawlow, A.L.; Siegel, A.; Wang, Z-Y.; Yan, G-Y.; Polarization intermodulated excitation (POLINEX) spectroscopy of helium and neon, Opt. Comm. 37: 87-91 (April 1981).
28. Demtröder, W.; Laser spectroscopy, 494-499 Springer-Verlag, Berlin (1982).
29. Bayer-Helms, F.; Helmcke, J.; Modulation broadening of spectral profiles, PTB-Bericht Me-17, Braunschweig, Germany (1977).
30. Little, C.E.; The interaction of stimulated emission and gain medium in the CO laser, Ph. D. Thesis, Macquarie University, Sydney Australia (1987).
31. George, T.; Saupe, S.; Wappelhorst, M.H.; Urban, W.; The CO fundamental band laser as a secondary frequency standard at 5 μm , submitted to Applied Phys.B (1994).
32. Tuma, W.; van der Hoeven, C.J.; Parallel movement piezoelectric transducer, Rev. Sci. Instrum. 47: 765-766 (June 1976).
33. Dax, A.; Präzisionsspektroskopie im Mittlern infraroten Spektralbereich, I Photoakustischer Nachweis von Methan, II Heterodynmessungen an OCS bei 87 THz, III Subdopplermethoden zur Ermittlung von Eichgaslinien, Ph. D. thesis, Inst. f. Angew. Physik, Univ of Bonn, Germany (1992).
34. Büscher, S.; Resonante Absorptionszellen für die Infrarotlaser-photoakustische Spektroskopie von Gasen, Diploma thesis, Inst. f. Angew. Physik, Univ. of Bonn, Germany (1991).
35. Müller, K.; Aufbau und Erprobung einer astigmatikuskomponensierten Whitzeile mit piezo unterstützter Etaloneliminierung, Diploma thesis, Inst. f. Angew. Physik, Univ. of Bonn, Germany (1993).
36. George, T.; Der CO-Fundamentalbanden Laser als sekundärer Frequenzstandard: hochauflösende Sättigungsspektroskopie und Heterodynfrequenzmessung an CO und OCS zwischen 1900 und 2100 cm^{-1} , Ph. D. thesis, Inst. f. Angew. Physik, Univ. of Bonn, Germany (1993).

37. Wieman, C.; Hänsch, T.W.; Doppler-free laser polarization spectroscopy, *Phys. Rev. Lett.* **36**: 1170-1173 (May 1976).
38. Stert, V.; Fischer, R.; Doppler-free polarization spectroscopy using linear polarized light, *Appl. Physics* **17**: 151-154 (Oct 1978).
39. Delsart, C.; Keller, J.C.; in *Laser Spectroscopy III*, Hall, J.L.; Carlsten, J.L., eds., Springer-Verlag, Berlin (1977).
40. Saikan, S.; Angular momentum dependence of laser-induced birefringence and dichroism in atomic resonance lines, *J. Opt. Soc. Am.* **68**(9): 1184-1187 (Sept 1978).
41. Goddon, D.; Groh, A.; Hanses, H.J.; Schneider, M.; Urban, W.; Heterodyne frequency measurements of the 1-0 band of HF at 2.7 μm , *J. Mol. Spectrosc.* **147**: 392-397 (June 1991).
42. Groh, A.; Goddon, D.; Schneider, M.; Zimmermann, W.; Urban, W.; Sub-Doppler heterodyne frequency measurements on the CO₂ 10⁰11-00⁰01 vibrational band: new reference lines near 3714 cm⁻¹, *J. Mol. Spectrosc.* **146**: 161-168 (Mar 1991).
43. Raab, M.; Höning, G.; Demtröder, W.; Vidal, C.R.; High resolution laser spectroscopy of Cs₂.II. Doppler free polarization spectroscopy on the C¹ $\Pi_u \leftarrow X^1\Sigma_g^+$ system, *J. Chem. Phys.* **76**(9): 4370-4386 (May 1982).
44. Levenson, M.D.; Eesley, G.L.; Polarization selective optical heterodyne detection for dramatically improved sensitivity in laser spectroscopy, *Appl. Phys.* **19**: 1-17 (April 1979).
45. Wieman, C.; Hänsch, T.W.; Precision measurement of the 1S Lamb shift and the 1S-2S isotope shift of hydrogen and deuterium, *Phys. Rev. A* **22**: 192-205 (July 1980).
46. Belfrage, Ch.; Grafström, P.; Kröll, S.; Svanberg, S.; Doppler-free laser spectroscopy measurements on a Ne discharge for determination of ²²Ne-²⁰Ne isotope shifts, *Physica Scripta* **27**: 367-370 (May 1983).
47. Raab, M.; Weber, A.; Amplitude-modulated heterodyne polarization spectroscopy, *J. Opt. Soc. Am. B.* **2**(9): 1476-1479 (Sept 1985).
48. Bohle, W.; Konzepte der Absorptionsspektroskopie mit Polarisierungseffekten, Internal report Inst. f. Angew. Physik, Univ. of Bonn, Germany (1989).

49. Keyes, R.J; ed., Optical and infrared detectors in "Topics in Applied Physics" 19: Springer-Verlag, Berlin (1977).
50. Azzam, R.M.A.; Ellipsometry and Polarized Light, North Holland Publ., Amsterdam (1977).
51. Murty, M.V.R.K.; Shukla, R.P.; Extinction of light in Brewster polarizers: a shadow phenomenon, Appl. Opt. 22: 1094-1098 (Apr 1983).
52. Chraplyvy, A.R.; Polarization flipper for infrared laser beams, Appl. Opt. 15: 2022-2023 (Sept 1976).
53. Born, M.; Principles of Optics, 6th ed., Pergamon Press, Oxford (1987).
54. Wolfe, W.L.; Zissis, G.J., eds.; The Infrared Handbook, Office of Naval Research, Washington DC (1978).
55. Wells, J.S.; Dax, A.; Hollberg, L.; Maki, A.G.; Sub-Doppler frequency measurements on OCS near 1689 and 1885 cm^{-1} , J. Mol. Spectrosc. (to be submitted).
56. Mürtz, M.; Schaefer, M.; Schneider, M.; Wells, J.S.; Urban, W.; Schiessl, U.; Tacke, M.; Stabilization of 3.3 and 5.1 μm lead-salt diode lasers by optical feedback, Optics Commun. 94: 551-556 (Dec 1992).
57. Maki, A.G.; Chou, C.C.; Evenson, K.M.; Zink, L.; Shy, J. T.; Improved molecular constants and frequencies for the CO_2 laser from new high- J regular and hot-band frequency measurements, J. Mol. Spectrosc. (accepted).
58. Bradley, L.C.; Soohoo, K.L.; Freed, C.; Absolute frequencies of lasing transitions on nine CO_2 isotopic species, IEEE J. Quantum Electron. QE-22: 234-267 (Feb 1986).

NIST Technical Publications

Periodical

Journal of Research of the National Institute of Standards and Technology—Reports NIST research and development in those disciplines of the physical and engineering sciences in which the Institute is active. These include physics, chemistry, engineering, mathematics, and computer sciences. Papers cover a broad range of subjects, with major emphasis on measurement methodology and the basic technology underlying standardization. Also included from time to time are survey articles on topics closely related to the Institute's technical and scientific programs. Issued six times a year.

Nonperiodicals

Monographs—Major contributions to the technical literature on various subjects related to the Institute's scientific and technical activities.

Handbooks—Recommended codes of engineering and industrial practice (including safety codes) developed in cooperation with interested industries, professional organizations, and regulatory bodies.

Special Publications—Include proceedings of conferences sponsored by NIST, NIST annual reports, and other special publications appropriate to this grouping such as wall charts, pocket cards, and bibliographies.

Applied Mathematics Series—Mathematical tables, manuals, and studies of special interest to physicists, engineers, chemists, biologists, mathematicians, computer programmers, and others engaged in scientific and technical work.

National Standard Reference Data Series—Provides quantitative data on the physical and chemical properties of materials, compiled from the world's literature and critically evaluated. Developed under a worldwide program coordinated by NIST under the authority of the National Standard Data Act (Public Law 90-396). NOTE: The Journal of Physical and Chemical Reference Data (JPCRD) is published bi-monthly for NIST by the American Chemical Society (ACS) and the American Institute of Physics (AIP). Subscriptions, reprints, and supplements are available from ACS, 1155 Sixteenth St., NW, Washington, DC 20056.

Building Science Series—Disseminates technical information developed at the Institute on building materials, components, systems, and whole structures. The series presents research results, test methods, and performance criteria related to the structural and environmental functions and the durability and safety characteristics of building elements and systems.

Technical Notes—Studies or reports which are complete in themselves but restrictive in their treatment of a subject. Analogous to monographs but not so comprehensive in scope or definitive in treatment of the subject area. Often serve as a vehicle for final reports of work performed at NIST under the sponsorship of other government agencies.

Voluntary Product Standards—Developed under procedures published by the Department of Commerce in Part 10, Title 15, of the Code of Federal Regulations. The standards establish nationally recognized requirements for products, and provide all concerned interests with a basis for common understanding of the characteristics of the products. NIST administers this program in support of the efforts of private sector standardizing organizations.

Consumer Information Series—Practical information, based on NIST research and experience, covering areas of interest to the consumer. Easily understandable language and illustrations provide useful background knowledge for shopping in today's technological marketplace.

Order the above NIST publications from: Superintendent of Documents, Government Printing Office, Washington, DC 20402.

Order the following NIST publications—FIPS and NISTIRs—from the National Technical Information Service, Springfield, VA 22161.

Federal Information Processing Standards Publications (FIPS PUB)—Publications in this series collectively constitute the Federal Information Processing Standards Register. The Register serves as the official source of information in the Federal Government regarding standards issued by NIST pursuant to the Federal Property and Administrative Services Act of 1949 as amended, Public Law 89-306 (79 Stat. 1127), and as implemented by Executive Order 11717 (38 FR 12315, dated May 11, 1973) and Part 6 of Title 15 CFR (Code of Federal Regulations).

NIST Interagency Reports (NISTIR)—A special series of interim or final reports on work performed by NIST for outside sponsors (both government and non-government). In general, initial distribution is handled by the sponsor; public distribution is by the National Technical Information Service, Springfield, VA 22161, in paper copy or microfiche form.

U.S. Department of Commerce
National Institute of Standards and Technology
325 Broadway
Boulder, Colorado 80303-3328

Official Business
Penalty for Private Use, \$300